01 Jan 2004

Analysis of Jet-Wing Distributed Propulsion from Thick Wing Trailing Edges

Serhat Hosder
Missouri University of Science and Technology, hosders@mst.edu

Joseph A. Schetz

Vance Dippold

Recommended Citation

S. Hosder et al., "Analysis of Jet-Wing Distributed Propulsion from Thick Wing Trailing Edges," *Proceedings of the 42nd AIAA Aerospace Sciences Meeting and Exhibit (2004, Reno, NV)*, American Institute of Aeronautics and Astronautics (AIAA), Jan 2004.
The definitive version is available at https://doi.org/10.2514/6.2004-1205

42nd AIAA Aerospace Sciences Meeting and Exhibit
5 - 8 January 2004, Reno, Nevada

AIAA 2004-1205

ANALYSIS OF JET-WING DISTRIBUTED PROPULSION FROM THICK WING TRAILING EDGES

Vance Dippold, III*, Serhat Hosder*, and Joseph A. Schetz†
Department of Aerospace and Ocean Engineering
Virginia Polytechnic Institute and State University
Blacksburg, VA 24061

Abstract

Conventional airliners use two to four engines in a Cayley-type arrangement to provide thrust, and the thrust is concentrated right behind the engine. Distributed propulsion is the idea of redistributing the thrust across most, or all, of the wingspan of an aircraft. This can be accomplished by using several large engines and using a duct to spread out the exhaust flow to form a jet-wing or by using many small engines spaced along the span of the wing. Jet-wing distributed propulsion was originally suggested as a way to improve propulsive efficiency. A previous study at Virginia Tech assessed the potential gains in propulsive efficiency. The purpose of this study was to assess the performance benefits of jet-wing distributed propulsion. The Reynolds-averaged, finite-volume, Navier-Stokes code GASP was used to perform parametric computational fluid dynamics (CFD) analyses on two-dimensional jet-wing models. The jet-wing was modeled by applying jet boundary conditions on the trailing edges of blunt trailing edge airfoils such that the vehicle was self-propelled. As this work was part of a Blended-Wing-Body (BWB) distributed propulsion multidisciplinary optimization (MDO) study, two airfoils of different thickness were modeled at BWB cruise conditions as examples. One airfoil, representative of an outboard BWB wing section, was 11% thick. The other airfoil, representative of an inboard BWB wing section, was 18% thick. Furthermore, in an attempt to increase the propulsive efficiency, the trailing edge thickness of the 11% thick airfoil was doubled in size. The studies show that jet-wing distributed propulsion can be used to obtain propulsive efficiencies on the order of turbofan engine aircraft. If the trailing edge thickness is expanded, then jet-wing distributed propulsion can give improved propulsive efficiency. However, expanding the trailing edge must be done with care, as there is a drag penalty.

---

* Graduate student, Student Member AIAA

† Fred D. Durham Chair, Fellow AIAA

Nomenclature

BWB	Blended-Wing-Body
TE	Trailing Edge
b	Wing span
b_{jet}	Span of jet-wing
c	Chord length
C_D	Drag coefficient
$C_{D_{net}}$	Net drag coefficient, includes jet thrust
C_J	Jet thrust coefficient
C_L	Lift coefficient
$C_{L_{net}}$	Net lift coefficient, includes jet thrust
C_p	Pressure coefficient
D	Drag
D_{Net}	Net drag, includes jet thrust
h_{jet}	Jet height
L_{Net}	Net lift, includes jet thrust
m	Jet flow mass
M_∞	Freestream Mach number
M_{jet}	Jet flow Mach number
p_∞	Freestream pressure
p_{jet}	Jet flow pressure
p_{TE}	Pressure at trailing edge
Re	Reynolds number
Re_c	Chord Reynolds number
S, S_{ref}	Jet reference area
$\frac{t}{c}$	Thickness ratio
$Thrust_{jet}$	Jet thrust
T_∞	Temperature of freestream
U_∞	Freestream velocity magnitude
U_{jet}	Jet velocity magnitude
α	Airfoil angle of attack
η_P	Froude propulsive efficiency
ρ_∞	Freestream density
ρ_{jet}	Jet flow density
τ	Jet deflection angle

Introduction

A major potential aerodynamic benefit of distributed propulsion lies in the ability to synergistically integrate the propulsion system and the airframe. Integrated propulsion/lift systems already exist in nature: birds and flying insects use their wings to produce both lift and thrust. As shown in Figure 1, the original jet-wing configuration by Kuchemann [1] incorporates the propulsion system into the aircraft by burying the engines in the wing and blowing the engine exhaust out of the trailing edge. Kuchemann‡ [2] proposes that the jet-wing arrangement may be more efficient than a conventional engine arrangement, in which the engine nacelles are located some distance away from the wing and body. See Reference [3] for more on that topic.

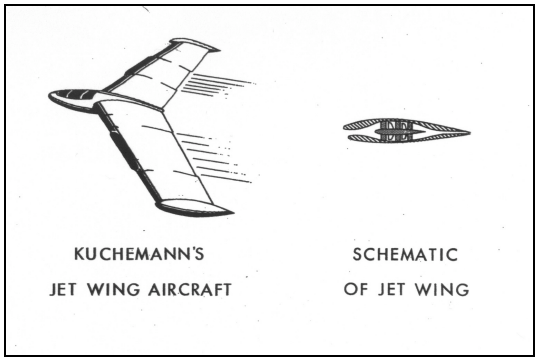

Figure 1: Kuchemann's jet-wing aircraft concept [1].

Distributed propulsion does have other potential benefits, one of which is improved safety due to engine redundancy. With numerous engines, the impact of an engine-out situation is reduced. Distributing the engine weight across a wing could possibly decrease gust load/flutter problems and provide passive load alleviation resulting in reduced wing weight. Also, smaller, easily-interchangeable engines can potentially result in improved affordability. In addition, one can envision a jet-

‡ The original reference to Kuchemann's introduction of the jet-wing concept has been cited as: "On the Possibility of Connecting the Production of Lift with that of Propulsion," *M.A.P. Volkenrode, Reports and Translations* No. 941-1 Nov., 1947, APPENDIX I, Kuchemann, D., "The Jet Wing." However, a copy of this reference could not be obtained.

wing with deflected jets replacing flaps and slats and the associated noise.

Kuchemann never performed any detailed studies with the jet-wing [1]. However, a number of analytical, numerical, and experimental studies have been performed on jet-flaps [4-8], which are similar to jet-wings. In contrast to jet-wings, which have small jet deflection angles and are associated with cruise situations, jet-flaps typically have large jet deflection angles and are found in high-lift applications. Only Yoshihara and Zonars [7] consider jet-flaps in viscous, transonic flow, but they considered only high-lift configurations; no cruise configurations were presented.

The purpose of this paper is to present numerical analyses of several self-propelled jet-wing models at cruise conditions in viscous, transonic flow. The goals of this study were to ascertain the effect of jet-wing distributed propulsion on propulsive efficiency, to observe how jet-wing distributed propulsion affects the flowfield around the airfoil, and to begin to consider design changes that might be implied.

The propulsive efficiency is improved because a jet exiting out the trailing edge of the wing 'fills in' the wake directly behind the wing. Propulsive efficiency loss is a consequence of any net kinetic energy left in the wake (characterized by non-uniformities in the velocity profile) compared to that of a uniform velocity profile. Naval architects implement this concept on ships and submarines by installing a propeller directly behind a streamlined body. This tends to maximize the propulsive efficiency of the ship-propeller system, even though the wake is typically not perfectly filled [9].

The Froude Propulsive Efficiency, η_P, is defined as the ratio of useful power out of the propulsor to the rate of kinetic energy added to the flow by the propulsor. For a jet engine isolated from an aircraft wing, the familiar result is:

$$\eta_P = \frac{2}{\frac{U_{jet}}{U_\infty} + 1} \qquad (1)$$

For a typical high-bypass-ratio turbofan at Mach 0.85, the Froude Propulsive Efficiency is about 80% [10].

Consider the distributed propulsion system shown in Figure 2, in which the jet and the wake of the body are combined. In the ideal system, the jet perfectly 'fills in' the wake, creating a uniform velocity profile. In this case, the kinetic energy added to the flow by the jet compared to that of a uniform velocity profile is zero, and the propulsive efficiency is $\eta_P = 100\%$. However, the jet does not fully 'fill in' the wake in practice, but creates smaller non-uniformities in the velocity profile, as illustrated in Figure 3. But, the resulting velocity profile contains a smaller net kinetic energy than that of the case where the body and engine are independent. Ko, Schetz, and Mason [3] present an analysis of the propulsive efficiency of a distributed propulsion system of this type. The efficiency of a distributed propulsion system will be bounded by the efficiency of the body/engine configuration (nominally 80%) and the perfect distributed propulsion configuration of 100%. Note, however, that the effect of the jet on the overall pressure distribution of the body was not included.

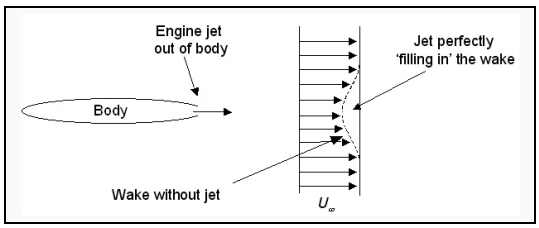

Figure 2: The velocity profile of a perfect distributed propulsion body/engine system [3].

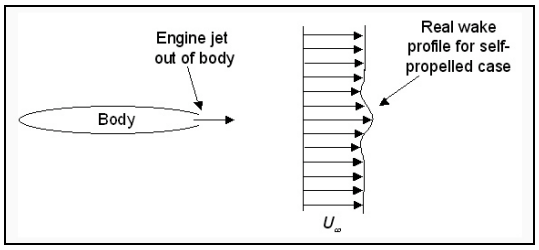

Figure 3: The velocity profile of a realistic distributed propulsion body/engine system [3].

Model and Method

Here, distributed propulsion theory is applied to a transonic passenger transport aircraft, where it is assumed supercritical airfoils are used. A major characteristic of supercritical airfoils is the presence of a thick trailing edge to reduce wave drag [11]. A typical trailing edge

thickness of a supercritical airfoil is approximately 0.7% of the airfoil chord length. A trailing edge of this size is large enough to accommodate channeling enough exhaust out to overcome the local drag due to viscous and pressure forces.

For this study, airfoils were developed to be representative of the wing sections found on a transport aircraft, more specifically, a Blended-Wing-Body (BWB) aircraft. The first airfoil, referred to as the "Outboard" airfoil, is representative of wing sections found on the outboard portion of a BWB having a thickness of $\frac{t}{c} = 11\%$, a design lift coefficient of $C_L = 0.69$, and a chord length of $c = 6.77\,\text{m}$. The Outboard airfoil was developed by modifying a SC(2)-0410 supercritical airfoil by adding small cubic bumps [12] along the upper surface and stretching the lower surface. The modifications were performed in order to reduce the shock strength and to reduce the aft loading. Complete details of the development process are found in Reference [13]. The pressure distribution of the Outboard and SC(2)-0410 airfoils were calculated with MSES Euler+Boundary Layer Code [14], [15] and are shown Figure 4. The final Outboard airfoil model is pictured in Figure 5. The Outboard airfoil has a trailing edge thickness of 0.49%.

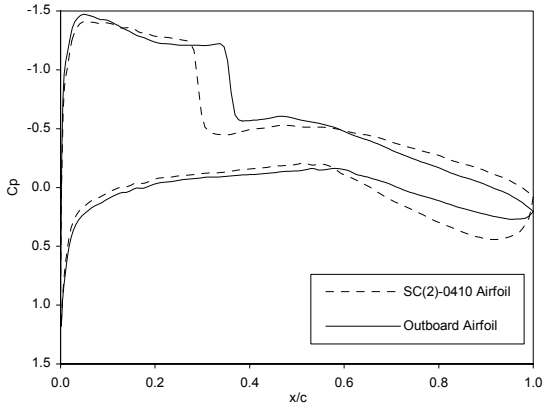

Figure 4: MSES pressure distributions of SC(2)-0140 and Outboard airfoils at $M_\infty = 0.72$, $C_L = 0.69$, $\text{Re}_c = 34.8e+6$.

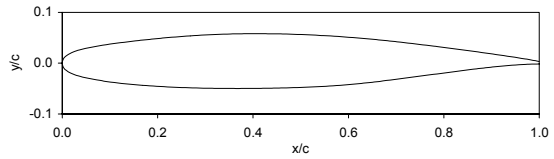

Figure 5: "Outboard" airfoil geometry.

A second airfoil was developed to be representative of the thicker inboard wing sections on a BWB aircraft. This "Inboard" airfoil is 18% thick, a chord length of 23.01 m, and a design C_L of 0.3. The Inboard airfoil was developed from a NACA 4-digit series airfoil with a thickness of $\frac{t}{c} = 18\%$, a maximum camber of 0.4%, and the maximum camber located at $\frac{x}{c} = 6\%$. The details of the modifications made can be found in Reference [13]. The Inboard airfoil geometry and pressure (from MSES) are shown in Figure 6 and Figure 7, respectively. The Inboard airfoil model has a 1% thick trailing edge.

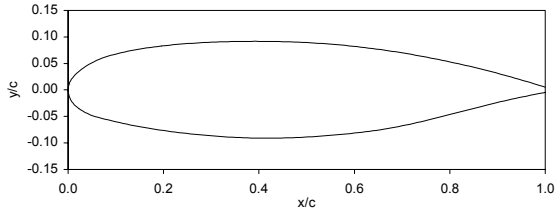

Figure 6: "Inboard" airfoil geometry.

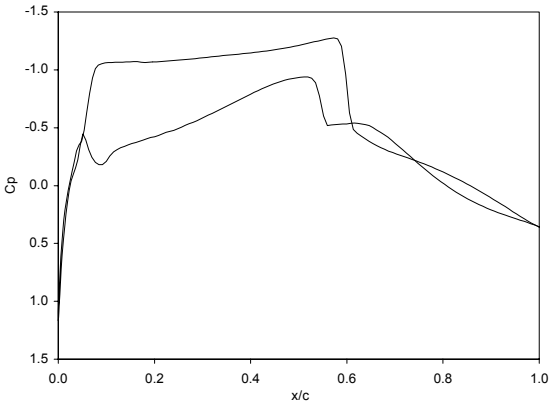

Figure 7: MSES pressure distribution of Inboard airfoil at $M_\infty = 0.72$, $C_L = 0.30$, $\text{Re}_c = 138.6e+6$.

One more airfoil development technique was performed in this research pursuit, namely expanding the trailing edge of the airfoil. One of the goals of the jet-wing distributed propulsion concept study is to increase the

propulsive efficiency of the aircraft. As will be discussed later, the propulsive efficiency of the baseline Outboard airfoil with the jet-wing applied was slightly lower than the 80% propulsive efficiency typical of turbofans [13]. Therefore, an attempt was made at decreasing the jet exit speed by increasing the height of the airfoil trailing edge. The trailing edge of the Outboard airfoil was expanded by truncating the airfoil at the location of desired trailing edge height and then linearly stretching the airfoil to the correct chord length. The trailing edge expansion of the Outboard airfoil increased the trailing edge height from 0.49% to 0.98% of the chord. The Outboard airfoil with the original trailing edge thickness is now referred to as the "Outboard 1xTE" airfoil, and the Outboard airfoil with the double thickness trailing edge is referred to as the "Outboard 2xTE" airfoil.

The computational analysis of the jet-wing models was performed using the Reynolds-averaged, three-dimensional, finite-volume, Navier-Stokes code GASP [10]. A total of six cases were run in GASP: a no-jet case and a jet-wing case for each of the three airfoil models. The three representative airfoils were each modeled using conventional two-zone C-grids, the details of which are described in detail in Reference [13]. The 300 by 64 grid for the Outboard 1xTE airfoil is shown in Figure 8 and Figure 9. The freestream flow properties specified in GASP for each of the three airfoils models are given in Table 1. For all three airfoil models, the GASP solution included all the viscous terms and used Menter's Shear Stress Transport $K-\omega$ turbulence model with compressibility corrections.

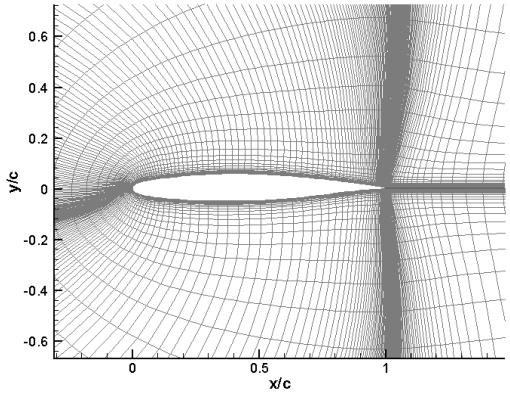

Figure 8: 2-zone grid of Outboard 1xTE airfoil (airfoil).

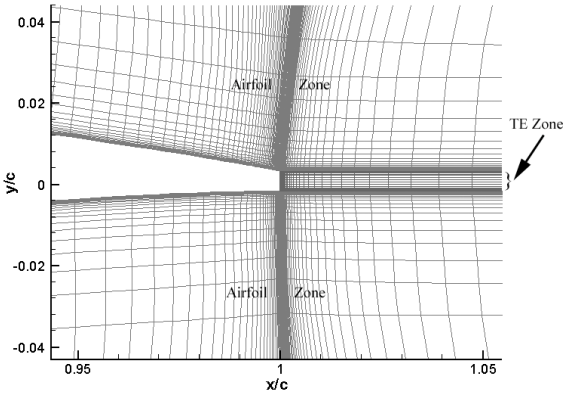

Figure 9: 2-zone grid of Outboard 1xTE airfoil (trailing edge).

Table 1: GASP freestream properties for representative airfoil models.

	Outboard 1xTE Airfoil	Outboard 2xTE Airfoil	Inboard Airfoil
Freestream Mach No., M_∞	0.72	0.72	0.75
Freestream Temp., T_∞	218.93 K	218.93 K	218.93 K
Freestream Density, ρ_∞	0.3807 kg/m^3	0.3807 kg/m^3	0.3807 kg/m^3
Angle of Attack, α	2.66°	3.00°	2.00°
Reynolds Number, Re_c	38.40e+6	38.40e+6	135.8e+6

The jet flow properties were determined using the results of the no-jet airfoil cases. To simplify the modeling, it was assumed that the jet would use exhaust from the engine fan and that it would be the same temperature as the freestream. Furthermore, the pressure of the jet flow was set equal to the average of pressures on the upper and lower surfaces of the airfoil at the trailing edge. The jet flow Mach number M_{jet} was determined from the thrust of the jet. Since the jet-wing is locally self-propelled, the jet thrust component in the freestream direction is equal to the drag:

$$\begin{aligned} Thrust_{jet} \cdot Cos(\alpha+\tau) &= D \\ Thrust_{jet} \cdot Cos(\alpha+\tau) &= C_D \cdot \left(\tfrac{1}{2} \cdot \rho_\infty \cdot U_\infty^2 \cdot c \cdot b\right) \end{aligned} \quad (2)$$

The jet thrust was found from the thrust equation:

$$Thrust_{jet} = \rho_{jet} \cdot U_{jet} \cdot h_{jet} \cdot \left(U_{jet} - U_{\infty}\right) + \left(p_{jet} - p_{\infty}\right) \cdot h_{jet} \quad (3)$$

After some manipulating,

$$\frac{C_D \cdot \left(\frac{1}{2} \cdot \rho_{\infty} \cdot U_{\infty}^2 \cdot c \cdot b\right)}{Cos(\alpha + \tau)} = \rho_{jet} \cdot U_{jet} \cdot h_{jet} \cdot \left(U_{jet} - U_{\infty}\right) + \left(p_{jet} - p_{\infty}\right) \cdot h_{jet} \quad (4)$$

Equation (4) was solved for the jet exit velocity, U_{jet}, and thus M_{jet}. The jet flow properties are listed in Table 2.

Table 2: GASP jet flow properties for representative jet-wing airfoil models.

	Outboard 1xTE Airfoil	Outboard 2xTE Airfoil	Inboard Airfoil
Drag Coefficient, C_D	0.0124	0.0136	0.0384
Jet Mach No., M_{∞}	1.199	1.021	1.385
Jet Temp., T_{∞}	218.93 K	218.93 K	218.93 K
Jet Density (Scaled), ρ_{∞}	0.4054 kg/m^3	0.4009 kg/m^3	0.4004 kg/m^3
Jet Angle, τ	0.0°	0.0°	0.0°

When no jet is present at the trailing edge, a no-slip boundary condition is applied to the trailing edge, just like the rest of the airfoil. However, when a jet is exhausted from the trailing edge, a Fixed-Q (not turbulence) boundary condition was applied. Q is defined by GASP [16] as the set of primitive variables. Flux splitting is disabled along the surface. This boundary condition is sufficient for a supersonic jet flow ($M_{jet} > 1$) and seems to have worked well for all the models (even when M_{jet} was very near 1).

The airfoil chordline is aligned with the x-axis in the Cartesian x-y coordinate system. The freestream flow, with velocity U_{∞}, is applied in GASP with an angle of attack α. Therefore, the lift and drag forces are aligned with a coordinate system rotated an angle α from the x-y coordinate system. Because only jet-wing cases are presented in this study, the jet flow, with velocity U_{jet}, exits the trailing edge of the airfoil with a jet deflection angle of $\tau = 0$.

The net force coefficients on the wing, including the effects of the jet thrust, were calculated:

$$C_{L_{Net}} = \frac{L_{Net}}{\frac{1}{2} \cdot \rho_{\infty} \cdot U_{\infty}^2 \cdot c \cdot b}$$
$$C_{D_{Net}} = \frac{D_{Net}}{\frac{1}{2} \cdot \rho_{\infty} \cdot U_{\infty}^2 \cdot c \cdot b} \quad (5)$$

The jet thrust coefficient, C_J, is defined as:

$$C_J = \frac{m \cdot U_{jet}}{\frac{1}{2} \cdot \rho_{\infty} \cdot U_{\infty}^2 \cdot S} \quad (6)$$

For the jet-wing to be self-propelled, the jet thrust coefficient, C_J, must be equal to the drag coefficient, C_D.

Results

Outboard 1xTE Airfoil

The GASP analysis showed that the Outboard 1xTE no-jet airfoil had a $C_L = 0.628$ and a $C_D = 0.0124$. The lift coefficient was 9% less than the target of $C_L = 0.69$.

From the results of the Outboard 1xTE no-jet airfoil case (C_D and p_{TE} in particular), the jet conditions were calculated that would produce a self-propelled jet-wing. The jet flow velocity required was $M_{jet} = 1.199$. Using Equation (1), the propulsive efficiency of the Outboard 1xTE jet-wing airfoil is $\eta_P = 75.1\%$. The resulting force coefficients and pressure distributions for the no-jet and jet-wing Outboard 1xTE airfoil are shown in Table 3 and Figure 10, respectively. It should be noted that it was necessary to increase the angle of attack by a small amount in order to compare the no-jet and jet-wing airfoils at the same net lift coefficient. The pressure distributions for the no-jet and jet-wing case at the same lift coefficient are nearly identical, even at the shock.

Table 3: Outboard 1xTE and 2xTE airfoil results.

Airfoil	Outboard 1xTE, no-jet	Outboard 1xTE, jet-wing	Outboard 2xTE, no-jet	Outboard 2xTE, jet-wing
Angle-of-attack, α	2.66°	2.75°	3.00°	3.13°
Jet Mach number, M_{jet}	0.000	1.199	0.000	1.021
Propulsive efficiency, η_P	--	75.1%	--	82.8%
Lift coefficient, C_L	0.6276	0.6208	0.6276	0.6350
Drag coefficient, C_D	0.0124	0.0117	0.0136	0.0121
Jet coefficient, C_J	0.0000	0.0115	0.0000	0.0122
Net lift coefficient, $C_{L_{Net}}$	0.6276	0.6230	0.6276	0.6389
Net drag coefficient, $C_{D_{Net}}$	0.0124	0.0002	0.0124	-0.0001

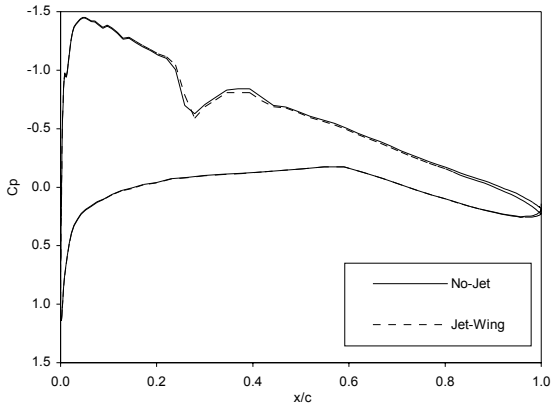

Figure 10: Outboard 1xTE no-jet and jet-wing airfoil pressure distributions for $C_{L_{Net}} = 0.63$.

Figure 11 shows the velocity profile 1% downstream of the airfoil. This helps to show why the propulsive efficiency is a bit low ($\eta_P = 75.1\%$) compared to typical high-bypass-ratio turbofan engine aircraft ($\eta_{P_{typical}} = 80\%$). The jet is rather thin ($\frac{h_{jet}}{c} = 0.49\%$) and does not do a good job of 'filling in' the wake behind the airfoil, and the jet velocity is much greater than the freestream velocity. Figure 12 shows the streamlines at the trailing edge of the Outboard 1xTE no-jet airfoil. A complex vortex forms on the trailing edge base when no jet is present. The flowfield of the Outboard 1xTE jet-wing airfoil is pictured in Figure 13. The jet-wing fills in the flow on the trailing edge base, and no vortex is present. The pressure contours in Figure 14 show that weak shocks and expansions do form in the jet. Still, it can be said that this is one of those rare cases when adding something to a flow problem actually simplifies the flowfield.

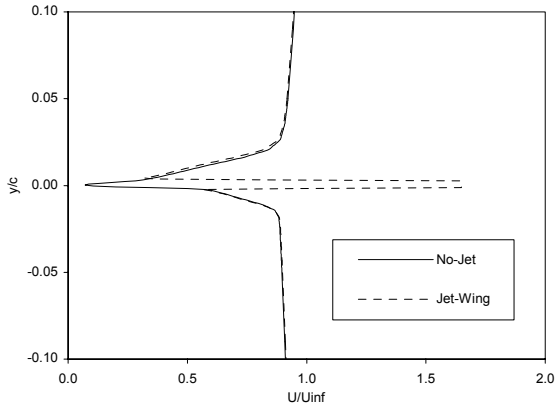

Figure 11: Velocity profile downstream of Outboard 1xTE no-jet and jet-wing airfoils, $\frac{x}{c} = 1.01$.

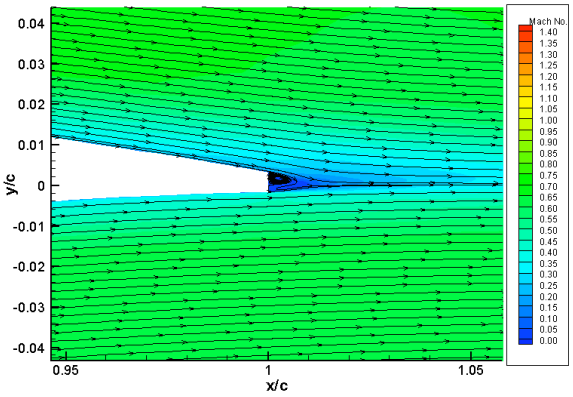

Figure 12: Streamlines and Mach number contours at trailing edge of Outboard 1xTE no-jet airfoil.

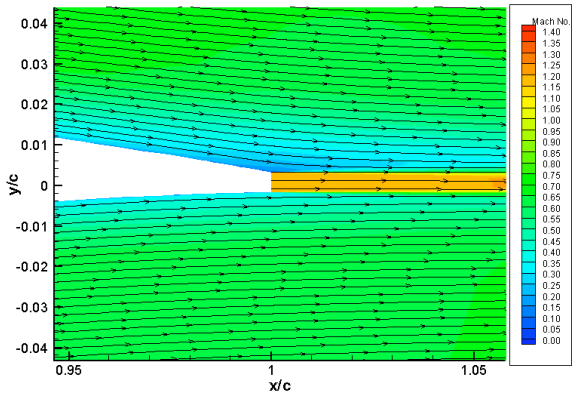

Figure 13: Streamlines and Mach number contours at trailing edge of Outboard 1xTE jet-wing airfoil.

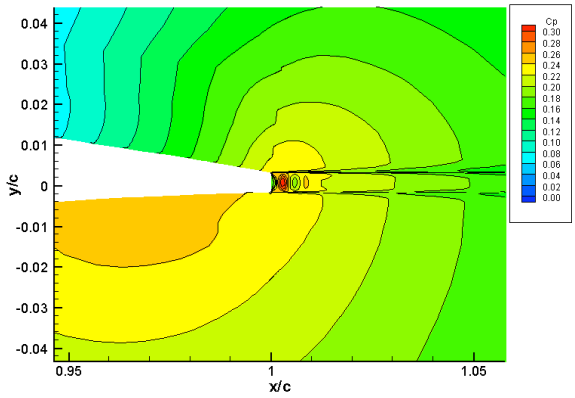

Figure 14: Pressure contours at the trailing edge of the Outboard 1xTE jet-wing airfoil.

Outboard 2xTE Airfoil

The next airfoil case studied was the Outboard 2xTE no-jet airfoil, for it was important to determine how this expanded trailing edge performs. As tabulated in Table 3, the drag of the Outboard 2xTE airfoil increases by 9.7% over the Outboard 1xTE airfoil. Although the net lift coefficients vary by only a small amount, the pressure distribution of the Outboard 2xTE airfoil, plotted in Figure 15, differs significantly from that of the Outboard 1xTE airfoil. The shock forms nearly 4% aft of where the shock forms on the Outboard 1xTE no-jet airfoil. The flowfield near the trailing edge of is pictured in Figure 16. Compared to the flowfield of the Outboard 1xTE no-jet airfoil in Figure 12, much larger vortex structures form on the base of the Outboard 2xTE airfoil.

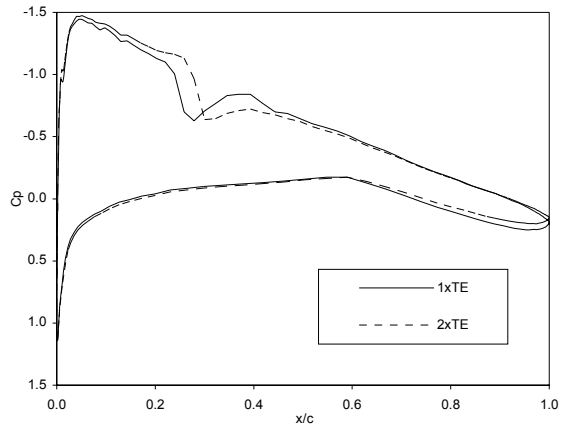

Figure 15: Outboard 1xTE and Outboard 2xTE no-jet airfoil pressure distributions for $C_{L_{Net}} = 0.63$.

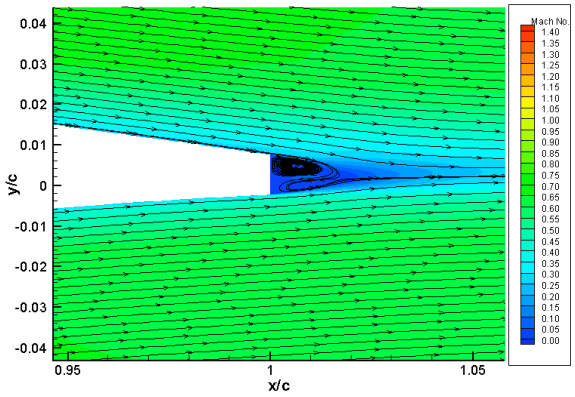

Figure 16: Streamlines and Mach number contours at trailing edge of Outboard 2xTE no-jet airfoil.

The results of the Outboard 2xTE no-jet case were used to calculate the required jet flow to produce a self-propelled vehicle. The required jet flow speed was $M_{jet} = 1.021$. The propulsive efficiency of the Outboard 2xTE jet-wing airfoil, calculated by Equation (2) is $\eta_P = 82.8\%$. The resulting force coefficients are tabulated in Table 3. The pressure distribution is pictured in Figure 17. As before, the jet-wing has a minimal effect on the pressure distribution. The velocity profiles in Figure 18 show why the propulsive efficiency has been increased. The Outboard 2xTE jet-wing has a lower speed than the Outboard 1xTE jet-wing, thus allowing it to better 'fill in' the wake behind the airfoil. The complex structure on the base of the Outboard 2xTE no-jet airfoil is eliminated by the jet, as shown in Figure 19. Figure 20 shows that the Outboard 2xTE jet-wing airfoil does not have the shock and

expansion structure of the Outboard 1xTE jet-wing airfoil.

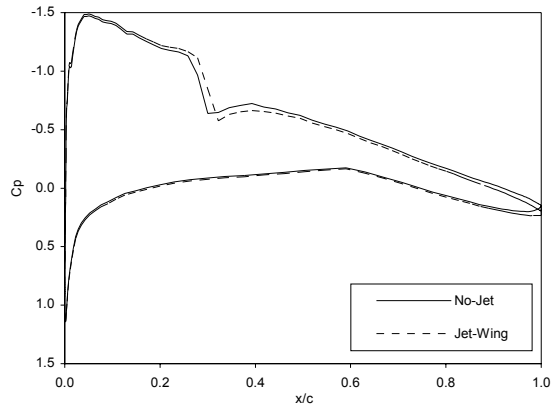

Figure 17: Outboard 2xTE no-jet and jet-wing airfoil pressure distributions for $C_{L_{Net}} = 0.63$.

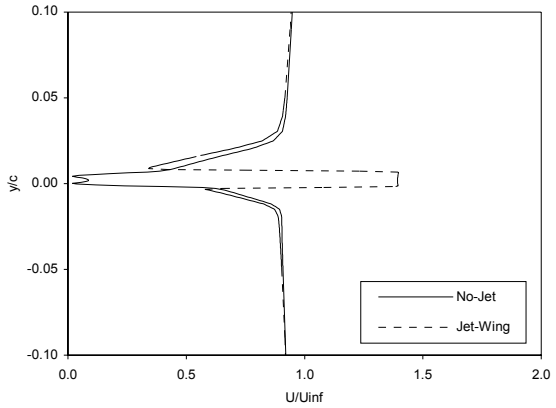

Figure 18: Velocity profile downstream of Outboard 1xTE and Outboard 2xTE jet-wing airfoils, $\frac{x}{c} = 1.01$.

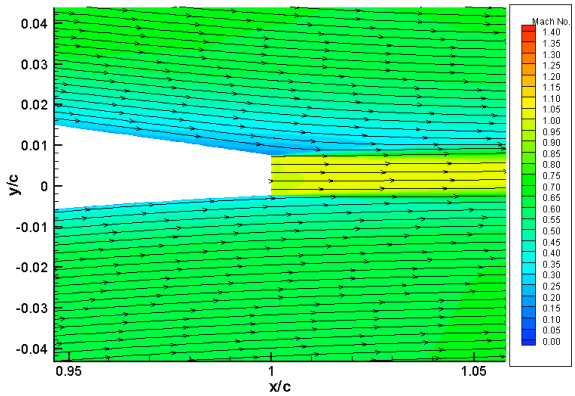

Figure 19: Streamlines and Mach number contours at trailing edge of Outboard 2xTE jet-wing airfoil.

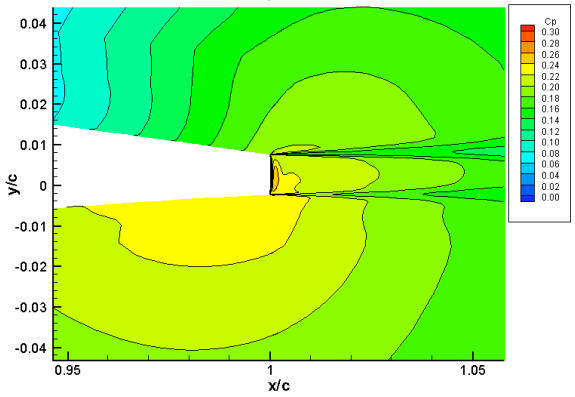

Figure 20: Pressure contours at the trailing edge of the Outboard 2xTE jet-wing airfoil.

For this airfoil of moderate thickness, when the trailing edge thickness (and jet height) is doubled, propulsive efficiency increases by 7.5%. However, the drag on the airfoil for the no-jet cases also increases substantially (nearly 10%). This could be a problem for an engine-out situation. Therefore, expanding the trailing edge height cannot simply be done arbitrarily.

Inboard Airfoil Results

The Inboard no-jet airfoil case presented several difficulties: the solution achieved an apparently periodic solution after 25,000 iterations, and the lift coefficient was well below the target lift coefficient of $C_L = 0.3$. MSES was used for the design of this airfoil, and that solution exhibited none of these difficulties. The solution oscillated between $C_{L_{Net}} = 0.032$ and $C_{L_{Net}} = 0.106$. Two approaches that could be used to eliminate the oscillations include running the solution until the oscillations damp out or computing the time-accurate solution. It was determined not to proceed with either. The first approach could be very computationally expensive, even if the oscillations ever damp out. The latter approach is beyond the scope of this parametric study, which is trying to find performance trends associated with jet-wing distributed propulsion. Therefore, the apparently periodic solution of the Inboard no-jet airfoil was analyzed by looking at the solutions at the "peaks" and "valleys" of the lift coefficient history tabulated in Table 4. The average lift coefficient of $C_L = 0.069$ is 77% less than the target lift coefficient of $C_L = 0.30$. The

Table 4: Inboard no-jet and jet-wing airfoil results.

Airfoil	Inboard no-jet "Peak"	Inboard no-jet "Valley"	Inboard, no-jet "Average"	Inboard, jet-wing (final)
Angle-of-attack, α	2.00°	2.00°	2.00°	2.00°
Jet Mach number, M_{jet}	0.000	0.000	0.000	1.385
Propulsive efficiency, η_P	--	--	--	70.3%
Lift coefficient, C_L	0.1056	0.0315	0.0685	0.2728
Drag coefficient, C_D	0.0277	0.0269	0.0273	0.0353
Jet coefficient, C_J	0.0000	0.0000	0.0000	0.0329
Net lift coefficient, $C_{L_{Net}}$	0.1056	0.0315	0.0685	0.2767
Net drag coefficient, $C_{D_{Net}}$	0.0277	0.0269	0.0273	0.0024

GASP solutions predict a region of separated flow beginning at $\frac{x}{c} = 88\%$. The GASP "peak" and "valley" solutions are shown in Figure 21.

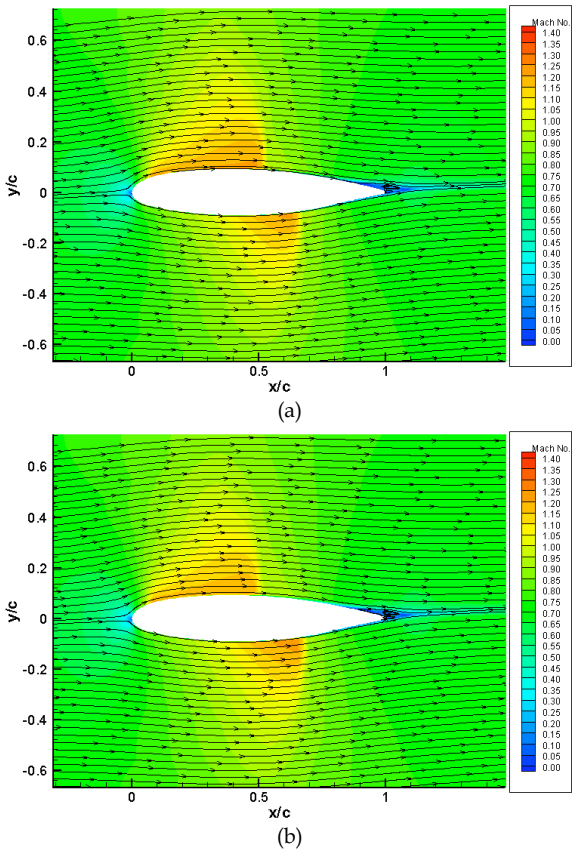

Figure 21: Streamlines and Mach number contours around Inboard no-jet airfoil: (a) "peak" solution, (b) "valley" solution.

The results show that this is a rather complex flow and that the Inboard airfoil may be a poor design. More design iterations are probably necessary to develop a good Inboard airfoil design, but each iterative cycle requires a substantial amount of time and effort.

The Inboard jet-wing airfoil was run based on results from the solution of the Inboard no-jet airfoil. Two iterations were required to obtain a self-propelled jet-wing vehicle. The jet flow Mach number of the final model was computed as $M_{jet} = 1.39$ using the drag coefficient of $C_D = 0.0384$. This high drag and high jet flow Mach number result in a rather low propulsive efficiency of $\eta_P = 70.3\%$. The force coefficient values are tabulated in Table 4 and it can bee seen that the vehicle is still not quite self-propelled, as the net drag coefficient was $C_{D_{Net}} = 0.0024$, which is within 7% of the airfoil drag. Unlike the Inboard no-jet airfoil case, the jet-wing airfoil cases converged without oscillations and to a lift coefficient of $C_{L_{Net}} = 0.277$, which is within 8% of the design lift coefficient of $C_L = 0.3$. The flowfield is shown in Figure 22. Figure 23 shows that the region of separation significantly affects the jet by creating a zone of low pressure and pulling the jet flow upwards. Lastly, the velocity profiles are plotted in Figure 24. The region of separation on the no-jet airfoil increases the size of the wake that a jet must 'fill in.' However, since the jet-wing airfoil also experiences a

region of separation, the jet does not do a good job of 'filling in' the wake downstream of the vehicle.

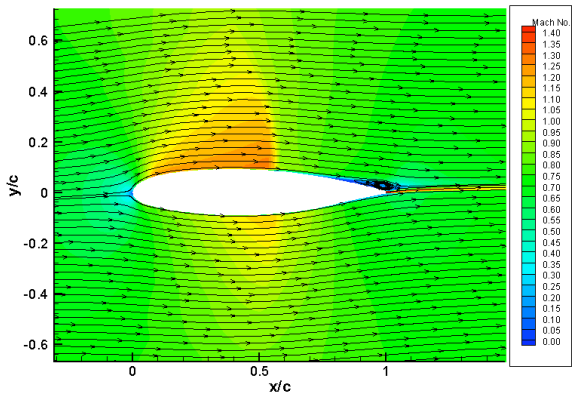

Figure 22: Streamlines and Mach number contours around Inboard jet-wing airfoil.

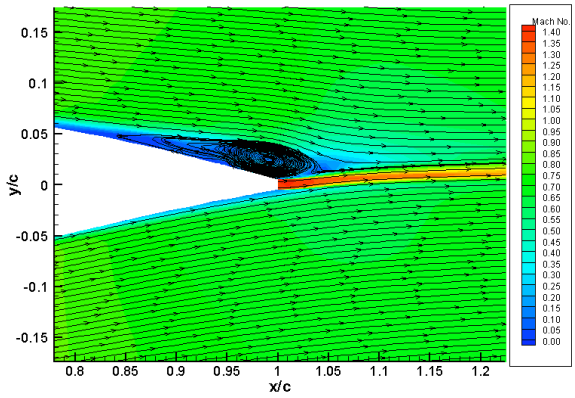

Figure 23: Streamlines and Mach number contours near trailing edge of Inboard jet-wing airfoil. Note region of separated flow.

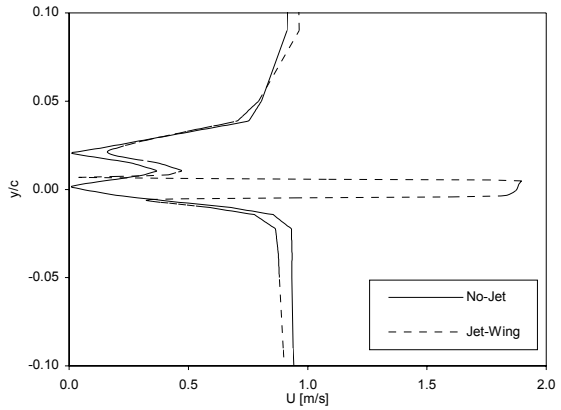

Figure 24: Velocity profile downstream Inboard no-jet "peak" and jet-wing airfoils.

Overall, the Inboard jet-wing airfoil exhibits more favorable results than the Inboard no-jet airfoil, particularly with respect to the lift coefficient, because it is much closer to the target of $C_L = 0.3$ than the Inboard no-jet airfoil. However, the inboard jet-wing airfoil still suffers a large region of separation (19% of the chord). While one might think that the jet-wing could entrain flow near the trailing edge and reduce the size of the region of separated flow, this is not the case. In fact, the region of separated flow grows larger with the presence of the jet-wing. This region of separated flow causes a large value of drag and a large wake that the jet-wing must 'fill in.' Therefore, the propulsive efficiency is rather low at $\eta_P = 70.3\%$. A better baseline design of the Inboard airfoil could be found, not only to reduce the drag and increase the propulsive efficiency when the jet-wing is applied, but also to give better performance when no jet is present.

Conclusions

Parametric CFD analyses were performed on two-dimensional jet-wing airfoils to assess the performance of the jet-wing in transonic, viscous flow. It has been suggested that distributed propulsion can increase propulsive efficiency beyond the $\eta_P = 80\%$ typical of modern turbofan-powered aircraft. This research effort attempted to validate this performance benefit of distributed propulsion and assess any negative consequences.

First, an airfoil was developed that was representative of the moderately thick wing sections at an outboard span location of the BWB. The jet-wing was applied to the Outboard 1xTE airfoil and the resulting propulsive efficiency was $\eta_P = 75\%$. Because the height of the jet was only 0.5% of the airfoil's chord and the wake had a height of about 4% of the chord, the jet did a poor job of 'filling in' the wake.

The trailing edge thickness – and thus the jet height – was then expanded to 1% of the chord. The propulsive efficiency increased to about $\eta_P = 83\%$. While this is a 3% increase over the propulsive efficiency of modern high-bypass-ratio aircraft, it must be remembered that the jet-wing is part of a hybrid distributed propulsion system, and the entire system's

propulsive efficiency must be taken into account. The drag of the Outboard 2xTE airfoil increased by nearly 10% over the drag of the Outboard 1xTE airfoil. While the increase in propulsive efficiency is favorable, the drag penalty is not. With a jet-wing, one cannot simply expand the jet height to a length approaching the size of the wake without negative aerodynamic consequences.

Performing CFD analyses on a thicker airfoil, representative of the thick inboard wing sections of a BWB aircraft, proved more complicated. The Inboard airfoil showed evidence of a periodic flow and lacked true steady-state convergence. This caused problems when applying the jet-wing. When the jet-wing was applied, the vehicle was not quite self-propelled. Only a small increase in the jet velocity is required to make the Inboard jet-wing airfoil self-propelled. The resulting propulsive efficiency would be $\eta_P = 69.7\%$. Unfortunately, the changes in lift and, in particular, drag could not be assessed for the Inboard airfoil, because the solution of the no-jet case was very much different from both the design and the jet-wing case. It can be concluded that the Inboard airfoil used may not be a good design and that a better baseline design should be used for future parametric CFD studies. Such work is now in progress. The current Inboard airfoil exhibits a more complex flowfield than the Outboard airfoil. This includes shocks on both surfaces and a region of separated flow that interact with each other and the jet-wing, when applied. The present studies show that the detailed design of an efficient jet-wing for inboard sections of the BWB represents a significant challenge that requires and deserves a concentrated effort.

Several recommendations can be made for future jet-wing distributed propulsion assessment work. It is recommended that a better Inboard airfoil design be developed. A better performing baseline Inboard airfoil would allow more confidence to be placed in the results of parametric CFD jet-wing studies.

One could look at designing airfoils with jet-wing propulsion in mind: airfoils with thicker trailing edges, but with low drag at cruise. One possible idea is a morphing wing, in which the aft portion can open and close, similar to many jet nozzles. When open, the trailing edge "nozzle" would provide high propulsive efficiency. During engine-out or when the engine thrust is not needed, the trailing edge would close to reduce drag.

These CFD studies were performed on two-dimensional models only, whereas distributed propulsion would ultimately be applied to a three-dimensional aircraft (be it a BWB or a conventional airliner). Therefore, it is recommended that CFD studies of jet-wing distributed propulsion be applied to a three-dimensional wing. As with all CFD analyses, these studies should begin low in complexity, i.e. a finite wing of simple taper and sweep with a jet-wing applied to the trailing edge.

Last, the control effectiveness of a jet-wing with deflected jets needs to be studied in detail with a view to eliminating flaps and slats and their associated noise.

Acknowledgements

This work was supported by the NASA Langley Research Center under Grant NAG-1-02024.

References

[1] Attinello, J. S., "The Jet Wing," IAS Preprint No. 703, IAS 25th Annual meeting, Jan. 28-31, 1957.

[2] Kuchemann, D., The Aerodynamic Design of Aircraft, Pergamon Press, New York, 1978, pp. 229.

[3] Ko, A., Schetz, J. A., Mason, W. H., "Assessment of the Potential Advantages of Distributed-Propulsion for Aircraft," XVIth International Symposium on Air Breathing Engines (ISABE), Cleveland, OH, Paper 2003-1094, Aug. 31 - Sept. 5, 2003.

[4] Hagendorn, H. and Ruden, P., "Wind Tunnel Investigation of a Wing with Junkers Slotted Flap and the Effect of Blowing Through the Trailing Edge of the Main Surface Over the Flap," Report by Institut fur Aeromachanik and Flugtechnik der Technischen Hochschule, Hannover LGL Bericht A64 (1938). Available as R.A.E. Translation No. 422, December, 1953.

[5] Spence, D. A., "The Lift Coefficient of a Thin, Jet-Flapped Wing," Proceedings of the Royal Society of London, Series A, Mathematical and Physical Sciences, Volume 238, Issue 112, Dec., 1956, pp 46-68.

[6] Ives, D. C., and Melnik, R. E., "Numerical Calculation of the Compressible Flow over an Airfoil with a Jet Flap," 7th AIAA Fluid and Plasma Dynamics Conference, AIAA-74-542, Palo Alto, CA, June 17-19, 1974.

[7] Yoshihara, H., Zonars, D., "The Transonic Jet Flap: A Review of Recent Results." ASE-751089, National Aerospace and Manufacturing Meeting, November 1975.

[8] Kimberlin, R. D., "Performance Flight Test Evaluation of the Ball-Bartoe JW-1 JetWing STOL Research Aircraft," Flight Testing in the Eighties: 11th Annual Symposium Proceedings of the Society of Flight Test Engineers, Aug 27-29, 1980.

[9] Marine Engineering, Vol. 1, Society of Naval Architects & Marine Engineers, Ed. Herbert Lee Seward, pp. 10-11.

[10] Hill, P. and Peterson, C., Mechanics and Thermodynamics of Propulsion, 2nd Ed., Addison-Wesley, New York, 1992.

[11] Harris, C. D., "NASA Supercritical Airfoils: A Matrix of Family Related Airfoils," NASA TP 2969, March 1990.

[12] Mason, W. H., Applied Computational Aerodynamics Text/Notes, Appendix E, Utility Codes, E.5, Bump, http://www.aoe.vt.edu/~mason/Mason_f/CAtxtAppE.html.

[13] Dippold, V. F., Numerical Assessment of the Performance of Jet-Wing Distributed Propulsion on Blended-Wing-Body Aircraft, Master's Thesis, Virginia Polytechnic Institute and State University, 2003. Available at http://etd.vt.edu September 2004.

[14] Drela, M., "A User's Guide to MSES 2.95," MIT Computational Aerospace Sciences Laboratory, Sept., 1996.

[15] Drela, M., "MSES Multi-element Airfoil Design/Analysis Software – Summary," http://raphael.mit.edu/projects%26research.html, Massachusetts Institute of Technology, MA, May, 1994.

[16] GASP Version 4.1.1 Reference Guide, Aerosoft, Inc, Blacksburg, VA.